Am J Physiol Renal Physiol 293: F1768–F1776, 2007.
First published October 3, 2007; doi:10.1152/ajprenal.00365.2007.

Association of VASP with TRPC4 in PKG-mediated inhibition of the store-operated calcium response in mesangial cells

Xiaoxia Wang,[1] Jennifer L. Pluznick,[2] Deann C. Settles,[3] and Steven C. Sansom[3]

[1]*Department of Nephrology, No. 6 Hospital, Shanghai Jiaotong University, Shanghai, China;* [2]*Department of Cellular and Molecular Physiology, Yale University School of Medicine, New Haven, Connecticut; and* [3]*Department of Cellular and Integrative Physiology, University of Nebraska Medical Center, Omaha, Nebraska*

Submitted 3 August 2007; accepted in final form 2 October 2007

Wang X, Pluznick JL, Settles DC, Sansom SC. Association of VASP with TRPC4 in PKG-mediated inhibition of the store-operated calcium response in mesangial cells. *Am J Physiol Renal Physiol* 293: F1768–F1776, 2007. First published October 3, 2007; doi:10.1152/ajprenal.00365.2007.—We tested the hypotheses that the NO-cGMP-PKG pathway mediates inhibition of the store-operated cation channel (SOC) in human glomerular mesangial cells (HMC) and that TRPC4, a molecular component of SOC in HMC, is associated with PKG-phosphorylated vasodilator-stimulated phosphoprotein (VASP). Using fura 2 ratiometry, we measured intracellular Ca^{2+} concentration $[Ca^{2+}]_i$ to determine whether sodium nitroprusside (SNP), an NO donor, and 8-Br-cGMP affected SOC-TRPC4 via PKG. We found that the SOC response in HMC was attenuated in the presence of 100 μM SNP, an NO donor, or 100 μM 8-Br-cGMP. Addition of DT-3 (2.5 μM), a specific PKG-1α inhibitor, reversed the effects of 8-Br-cGMP on the SOC response. Application of 100 μM cAMP did not significantly inhibit the SOC response. RT-PCR and Western blotting revealed PKG-1α transcript and protein in HMC. Immunocytochemical analysis localized PKG-1α to the cytoplasm and plasma membrane of HMC. Previous studies have shown that PKG-mediated phosphorylation of VASP attenuates cellular Ca^{2+} entry, resulting in altered growth and proliferation. Therefore, we used Western blotting and immunocytochemistry to determine whether PKG-phosphorylated VASP associates with TRPC4. Western blot analysis revealed that 8-Br-cGMP enhanced the phosphorylation of VASP at serine 239 (Ser239), a known PKG phosphorylation site, in HMC within 5 min. Coimmunoprecipitation and coimmunostaining showed that P-Ser239-VASP associated with TRPC4. However, VASP that was unphosphorylated at Ser239 was not associated with TRPC4. These results indicate that VASP has a role in the NO/PKG-1α-mediated inhibition of the TRPC4-SOC response in HMC.

cGMP; SOC; nitric oxide; SNP

GLOMERULAR MESANGIAL CELLS are smooth muscle-like cells that surround the filtration capillaries of the glomerulus. Mesangial cells respond to cytokines and other pathogens of chronic renal disease by proliferating and secreting an extracellular matrix that ultimately compromises glomerular filtration rate (1, 9, 62). Within the glomerulus, at least two isozymes of NOS are present: mesangial cells contain inducible nitric oxide synthase (iNOS) (51), and glomerular endothelial cells contain endothelial NOS (27). Under various conditions, these NOS isoforms generate nitric oxide (NO), which can have either deleterious or beneficial effects on renal function. Excess glomerular generation of NO may contribute to the hyperfiltration often characteristic of early type 1 and type 2 diabetes mellitus (32). On the other hand, NO reduces proliferation and mesangial matrix deposition in response to TGF-β (10) or stretch-activated protein kinases (28). In cultured vascular smooth muscle cells, which are phenotypically similar to mesangial cells, the NO-cGMP-kinase pathway is antiproliferative (15, 18), prevents dedifferentiation, and slows angiotensin II-induced migration (16). Several studies have shown that the antimitogenic effect of NO is due to suppression of mitogen-induced transcription factors (21, 38, 47).

The role of intracellular Ca^{2+} in the activation of transcription factors has been well described in past studies (13, 19, 48). Proliferating cells require elevated concentrations of cytoplasmic Ca^{2+} and sarcoplasmic reticulum Ca^{2+} stores (23, 50), which are necessary for the activation of downstream Ras/ERK signaling pathways (43). That second messenger-operated channels were responsible for EGF-stimulated Ca^{2+} influx was shown initially by Sawyer and Cohen (49). It was subsequently found that Ca^{2+} entry is necessary for progression of the cell cycle (17, 33, 50). Thus the activation of plasmalemmal Ca^{2+} channels ensures an adequate concentration of intracellular and perhaps nuclear Ca^{2+} for the functioning of the enzymes that are stimulated in the process of proliferation.

Store-operated Ca^{2+} channels (SOC), activated on depletion of endoplasmic reticulum (ER) calcium stores, are formed by Orai proteins (20), which express as Ca^{2+}-selective ion channels (I_{CRAC}), or members of the TRPC subfamily, nonselective cation channels that are a branch of the transient receptor potential (TRP) superfamily of cation channels. The signal from the depletion of calcium from ER stores to the activation of SOC is mediated by STIM1 (37, 46), which acts as a molecular messenger between the ER and SOC in mesangial cells (66), associates with TRPC1, TRPC4, and TRPC5, and appears to regulate their function as SOC (65).

In mesangial cells, SOC are composed of TRPC4 (60) and probably TRPC1 molecules (14, 53). It is now recognized that dysfunctional regulation of TRPC channels can result in cellular dedifferentiation and proliferative pathology. A recent study suggests that the dysfunctional regulation of TRPC6 channels plays a role in the development of renal failure resulting from focal segmental glomerulosclerosis (45).

Several studies have shown that cGMP regulates Ca^{2+} signaling and SOC activity in a negative manner (2, 5, 35). cGMP inhibits proliferation of colon cancer cells by inhibiting

Address for reprint requests and other correspondence: S. Sansom, Dept. of Cellular and Integrative Physiology, Univ. of Nebraska Medical Center, Omaha, NE (e-mail: ssansom@unmc.edu).

The costs of publication of this article were defrayed in part by the payment of page charges. The article must therefore be hereby marked "*advertisement*" in accordance with 18 U.S.C. Section 1734 solely to indicate this fact.

SOC (31). Thus cGMP is part of a second messenger pathway that attenuates SOC and prevents cellular proliferation and dedifferentiation of a variety of cell types.

Vasodilator-stimulated phosphoprotein (VASP), abundantly expressed in mesangial cells (22, 26), plays an important role in the regulation of cytoskeletal dynamics and cell migration (36, 44). Fibroblasts derived from $VASP^{-/-}$ mice exhibit increased motility, suggesting that VASP inhibits cell migration (3, 40). There are two major phosphorylation sites on VASP. Serine 157 (Ser157) is PKA specific, whereas serine 239 (Ser239) is specific for PKG. Phosphorylation of VASP at Ser239 by PKG inhibits growth of vascular smooth muscle (7), in part, by capping actin filaments, resulting in filament retraction (24).

VASP and SOC are both involved in cellular dedifferentiation and cellular migration in various cells. The experiments performed in this study were designed to investigate two hypotheses: *1*) the NO-cGMP-PKG axis mediates an attenuation of TRPC4-mediated Ca^{2+} entry in HMC, and *2*) phosphorylation of VASP at Ser239 causes its association with TRPC4 in the plasma membrane. This study could lead to establishing a role for the phosphorylation state of VASP to govern calcium entry via SOC channels.

METHODS

Culture of mesangial cells. Human glomerular mesangial cells (HMC) were cultured (8, 55) in DMEM, with 10 mM HEPES (pH = 7.4), 2.0 mM glutamine, 0.66 U/ml insulin, 1.0 mM sodium pyruvate, 0.1 mM nonessential amino acids, 100 U/ml penicillin, 100 μg/ml streptomycin, and 20% fetal bovine serum. When the cells reached confluency, they were passed onto 22 × 22 coverslips and studied within 56 h. All experiments employed HMC in *passages 6–10*. We found no differences in SOC activity within this span of passages.

Fura 2 fluorescence. Intracellular Ca^{2+} concentration ($[Ca^{2+}]_i$) was measured using the fura 2 fluorescence method of dual excitation wavelength microscopy, as previously described (25, 39). Briefly, cells were incubated for 60–90 min in physiological saline solution (PSS) containing 135 mM NaCl, 5 mM KCl, 2 mM $MgCl_2$, 1 mM $CaCl_2$, 10 mM HEPES, 7 μM fura 2 (fura 2-AM, 50 ug), 0.09 g/dl DMSO, and 0.018 g/dl Pluronic F-127 (Molecular Probes, Eugene, OR). For some cell preparations, either sodium nitroprusside (SNP; 100 μM), 8-bromo-cGMP (8-Br-cGMP; 100 μM) or 8-Br-cGMP plus DT-3 (2.5 μM) were added 15 min before the start of the Ca^{2+} measurement. After loading with fura 2, HMC were placed on the stage of a Nikon Diaphot-300 inverted microscope and perfused with PSS. The cells were then illuminated alternately at excitation wavelengths of 340 and 380 nm (bandwidth = 3 nm) with light from a DeltaScan dual monochromator system (Photon Technology International, Monmouth Junction, NJ). To limit detection of emitted fluorescence to a single cell (510 nm; 20-nm band pass), an adjustable optical sampling window was positioned within the path of light before detection by a photon-counting photomultiplier. Background-corrected data were collected at a rate of 5 points/s, stored, and analyzed using the Felix Software Package (Photon Technologies). Calibration of the fura 2 signal was done as previously described (25, 39). The addition of EGTA reduced the bath $[Ca^{2+}]$ to less than 10 nM.

Store-operated channel activity was measured as previously described in our laboratory (39). In brief, after a stable baseline $[Ca^{2+}]_i$ was obtained, 1 μM thapsigargin was applied to the bathing solution containing 1 mM Ca^{2+}. After an initial rapid rise and subsequent plateau phase, the bath $[Ca^{2+}]$ was reduced to <10 mM with EGTA. When $[Ca^{2+}]_i$ declined to the lowest level, 1 mM Ca^{2+} was returned to the bath. Once added, thapsigargin was present throughout the experiment. The difference in $[Ca^{2+}]_i$ ($\Delta[Ca^{2+}]_i$) in response to the return to the 1 mM Ca^{2+} to the external solution was the measure of SOC.

RT-PCR. For RT-PCR analysis of PKG-1α RNA, HMC were grown in DMEM supplemented with 5% FBS on 100-mm dishes and washed twice in PSS. Total RNA of HMC was extracted with TRIzol Reagent (GIBCO/BRL). Total RNA (2 μg) was reverse-transcribed by SuperScript III RNase H reverse transcriptase (Invitrogen). The primer pairs used for PKG-1α were 5′-TTCCGGAAGTTCACCAAGTC-3′ (forward) and 5′-AGAGTCTTGACGGTCGCTGT-3′ (reverse; GenBank accession no. D45864). The reaction conditions were as follows: 94°C (5 min); 35 cycles of 94°C (30 s), 58°C (1 min), 72°C (1 min); and 72°C (7 min). The RT-PCR products were run on a 1% agarose gel and visualized under a UVP imager.

Western blot analysis of PKG-Iα, P-Ser-TRPC4, and P-Ser239-VASP. Western blotting was used for the detection of PKG-1α and P-Ser239-VASP. For the detection of PKG-1α, total protein was isolated from confluent HMC. To analyze the 8-Br-cGMP-induced phosphorylation of VASP, confluent HMC were serum deprived (0.5% FBS DMEM) for 48 h and then exposed to 8-Br-cGMP (100 μM) at different time intervals. For Western analysis of both PKG-1α and P-Ser239-VASP, the cells were washed twice in ice-cold PBS and incubated for 30 min on ice in lysis buffer containing 10 mM Tris·HCl (pH 7.4), 100 mM NaCl, 1 mM EDTA, 1 mM EGTA, 1 mM NaF, 20 mM $Na_4P_2O_7$, 2 mM sodium vanadate, 1% Triton X-100, 10% glycerol, 0.1% SDS, 0.5% deoxycholate, 1 mM phenylmethylsulfonyl fluoride, and a proteinase inhibitor cocktail. After sonication, cell lysates were centrifuged at 12,500 *g* for 25 min at 4°C. The supernatant was collected, and protein concentration was determined using the BSA protein assay. For each lane, 50 μg of total protein in 2× sample buffer was boiled for 3∼5 min and then subjected to a 12.5% of SDS-PAGE followed by transfer to a polyvinylidene difluoride membrane. The blot was incubated with blocking buffer (5% nonfat dry milk in TBS-Tween 20 buffer) for 1 h at room temperature.

Phosphorylation of TRPC4 was analyzed using anti-phosphoserine (Sigma) after HMC were serum starved (0.5% FBS DMEM) and treated with 100 μM 8-Br-cGMP for 5, 10, 15, and 30 min.

The primary antibodies for P-Ser239-VASP (mouse anti-P-Ser239-VASP monoclonal IgG, 1 μg/ml, Upstate) and PKG-1α (goat anti-PKG-1α polyclonal IgG, 1:200, Santa Cruz) were applied to probe the membranes overnight at 4°C. The blots were washed for 5 min three times in TBS-Tween 20 at room temperature and then incubated with horseradish peroxidase (HRP)-conjugated goat anti mouse IgG, (1:2,500, Pierce) for P-Ser239-VASP and HRP-conjugated donkey anti-goat IgG (1:5,000, Santa Cruz) for PKG-1α (1 h at room temperature). The membrane was washed three times in TBS-Tween 20, exposed to the Supersignal West Femto Substrate (Pierce), and visualized under the UVP imager. For detection of VASP and internal control (β-actin), the membrane was stripped in stripping buffer for 15 min at 37°C and reprobed separately with primary antibodies (goat anti-VASP polyclonal IgG, 1:200 and goat anti-actin polyclonal IgG, 1:200, Santa Cruz.) The secondary antibody was donkey anti-goat HRP-conjugated IgG (1:5,000, Santa Cruz).

Immunocytochemical staining. For immunocytochemical staining, human mesangial cells were grown on sterile glass coverslips. Cells were washed twice in PSS and fixed with 4% formaldehyde for 15 min at room temperature, followed by being thoroughly rinsed three times with PBS. Permeabilization was carried out with methanol for 10 min at room temperature. After being washed three times with PBS, cells then were incubated with 1% BSA in PBS for 1 h at room temperature to block nonspecific binding sites. This was followed by incubation with goat anti-PKG-Iα (1:50, Santa Cruz), rabbit anti-P-Ser239-VASP (1:50. Upstate), rabbit anti-VA (1:50, Abcam or goat anti-Trpc4 (1:50, Santa Cruz) overnight at 4°C. Nonimmune goat and rabbit IgG were applied in place of the primary antibody for negative controls. Cells were then washed three times and then incubated with Alexa-488 conjugated donkey anti-goat IgG (1:400, Santa Cruz),

Alexa-594-conjugated donkey anti-goat, or Alexa-488-conjugated donkey anti-rabbit for 1 h at room temperature, followed by nuclear staining with Hoechst 33258 for 10 min at room temperature. After being washed three times, the cells were mounted with mounting media and viewed with a Leica fluorescent microscope. Pictures were taken with an Optronics digital camera.

Coimmunoprecipitation. Human glomerular mesangial cells were grown in the DMEM medium supplemented with 5% FBS until the cells reached confluence. After being serum starved for 48 h (0.5% DMEM), HMC (P6 ~ P9) were treated with 8-Br-cGMP (100 μM) in 10 mM Tris for 10 min. HMC were then harvested in the lysis buffer (100 mM NaCl, 1 mM EDTA, 1 mM EGTA, 1 mM NaF, 20 mM $Na_4P_2O_4$, 2 mM sodium vanadate, 1% Triton X-100, 1 mM PMSF, 10% glycerol, 0.5% deoxycholate). Five hundred micrograms of total cell lysates were incubated with mouse monoclonal P-Ser239-VASP IgG (1 μg/ml, Upstate) overnight at 4°C, followed by pull-down with washed protein G agarose beads 40 μl (Upstate) for 2 h at 4°C. For a negative control, the cell lysates were incubated with protein agarose G beads in the absence of anti-P-Ser239-VASP IgG. The cell lysates were separated by running a 7.5% acrylamide gel, followed by transferring of the separated protein on the polyvinylidene difluoride membrane. Immunoblotting was probed with polyclonal goat TRPC4 IgG (1 μg/ml, Santa Cruz). Regular Western blot analysis for TRPC4 was performed as a positive control. The results were visualized by incubating the blot with HRP-conjugated donkey anti-goat IgG (1:5,000, Santa Cruz) and developing the pictures with Supersignal West Femto Substrate (Pierce). The experiments were duplicated.

To determine whether unphosphorylated VASP associated with TRPC4, the HMC were serum starved for 48 h, placed in either 8-Br-cGMP or control media for 10 min, and lysed. The lysates were placed in a column that contained anti-VASP antibody (1:20, Calbiochem) and incubated at 4°C overnight. The anti-VASP antibody is specific only for unphosphorylated VASP. The unbound protein, final wash, and three elutions of the bound protein were run through a gel and stained using the Coomassie protein stain to detect any proteins present in the samples. The samples were then analyzed using a Western blot procedure and blotted with either TRPC4 antibody (1:200, Santa Cruz) or VASP antibody (1:200, Santa Cruz).

Materials. Thapsigargin, 8-Br-cGMP, and DT-3 were obtained from Calbiochem with 8-Bromo cGMP (100 μM) in 10 mM Tris for 10 min. SNP was obtained from Sigma.

Statistical analysis. Differences among data groups was determined by using one-way ANOVA plus a Student-Newman-Keuls test, with $P < 0.05$ being considered significant. Data are reported as means ± SE; n = number of cells.

RESULTS

Effects of NO-cGMP signaling on SOC. The fura 2 ratiometric method of measuring $[Ca^{2+}]_i$ was used to determine the effects of NO and the cGMP second messenger pathway on the SOC activity of HMC. Figure 1 shows representative tracings of $[Ca^{2+}]_i$, demonstrating the effects of SNP, 8-Br-cGMP, and

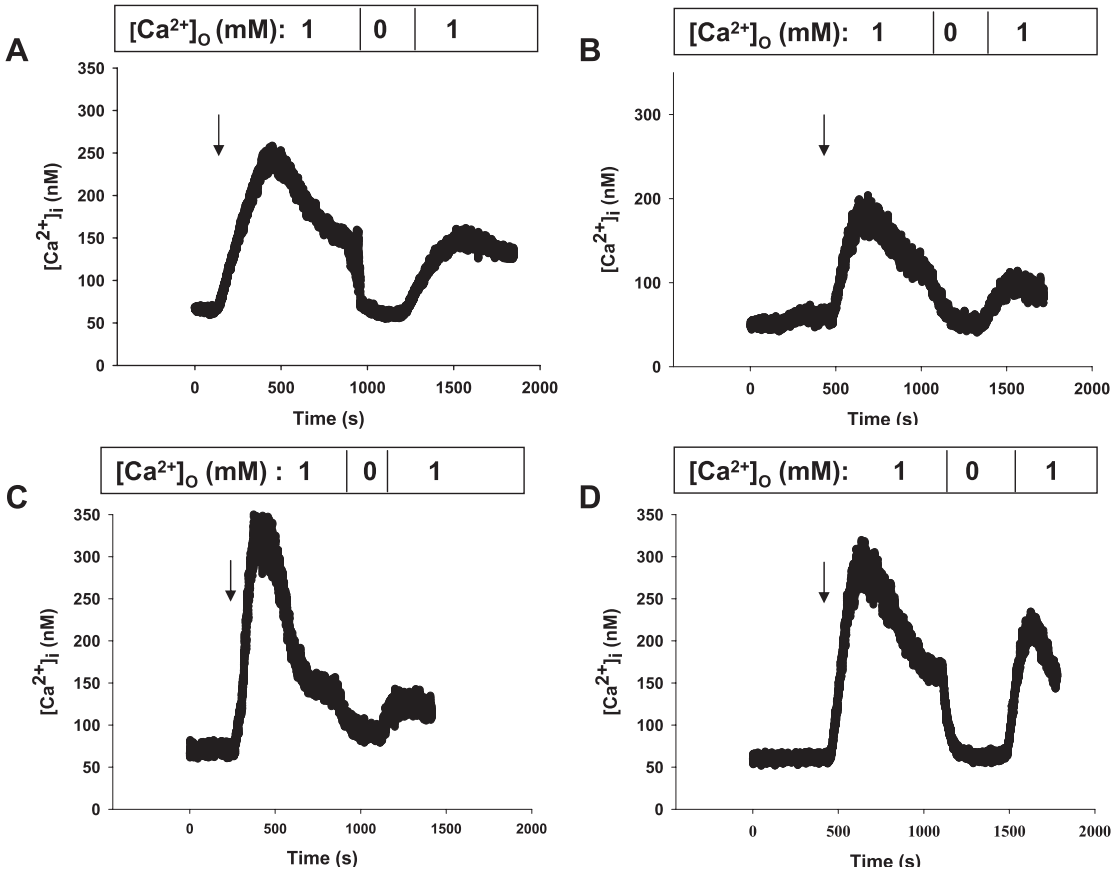

Fig. 1. Representative intracellular Ca^{2+} concentration ($[Ca^{2+}]_i$) recordings demonstrating control (*A*), effects of SNP (*B*), 8-bromo (Br)-cGMP (*C*), and 8-Br-cGMP+DT-3 (*D*). In each experiment, $[Ca^{2+}]_i$ increased from a baseline concentration to a peak when 1 μM thapsigargin, an inhibitor of SERCA, was added. After $[Ca^{2+}]_i$ declined from a peak value, extracellular Ca^{2+} concentration ($[Ca^{2+}]_o$) was reduced from 1 mM to <10 nM. When $[Ca^{2+}]_i$ decreased to its lowest value, 1 mM Ca^{2+} was returned to the external solution. The resulting increase in $[Ca^{2+}]_i$ was the measure of store-operated cation channel (SOC) activity.

8-Br-cGMP+DT-3. In the control experiment (Fig. 1*A*), $[Ca^{2+}]_i$ increased from a baseline concentration of 70 nM to a peak of 250 nM when 1 μM thapsigargin, an inhibitor of SERCA, was added to the bathing solution. When $[Ca^{2+}]_i$ was declining from a peak value, the extracellular Ca^{2+} concentration was reduced from 1 mM to <10 nM. When $[Ca^{2+}]_i$ decreased to its lowest value (typically near or slightly below the initial baseline), 1 mM Ca^{2+} was returned to the external solution. The resulting increase in $[Ca^{2+}]_i$ (i.e., 105 nM = 65–170 nM in control) was the measure of SOC activity. Figure 1*B* shows the effects of SNP (10 μM) added 15 min before the application of thapsigargin. In the presence of SNP, thapsigargin evoked an increase in $[Ca^{2+}]_i$ of 130 nM (from 70 to 200 nM), and the SOC response was 50 nM (from 60 to 110 nM). These values were, respectively, 28 and 52% less than control. As shown in Fig. 1*C*, the application of 100 μM 8-Br-cGMP 10 min before measurement of $[Ca^{2+}]_i$, reduced the SOC response by 80% to a value of 15 nM. Application of Br-cGMP plus DT-3 (1D), a peptide inhibitor of PKG-1α, resulted in an SOC response near the control value of 100 nM.

The illustrated experiment (see Fig. 1*B*) showed a lower magnitude of the thapsigargin-evoked release of Ca^{2+} from ER stores in the presence of NO. However, because the variability of the decrease was large, this effect did not reach statistical significance.

The bar graph in Fig. 2 summarizes the effects of SNP, 8-Br-cGMP, 8-Br-cGMP plus DT-3, and 8-Br-cAMP on the SOC response. All values represent increases in $[Ca^{2+}]_i$ from baseline. The SOC response ($[\Delta Ca^{2+}]_i$,) which was 110 ± 10 nM in control, was significantly attenuated to 55 ± 10 nM (n = 8) in the presence of SNP. Similarly, application of 8-Br-cGMP reduced SOC to a mean value of 58 ± 15 nM (n = 9), which was also significantly less than control. Addition of DT-3 (2.5 μM)+100 μM 8-Br-cGMP reversed the effects of 8-Br-cGMP to a value of 115 ± 10 nM, which was significantly greater than the mean values for the effects of SNP and 8-Br-cGMP on SOC, but not different from the control value. Application of 100 μM 8-Br-cAMP did not significantly reduce the SOC response (95 ± 20 nM, n = 5).

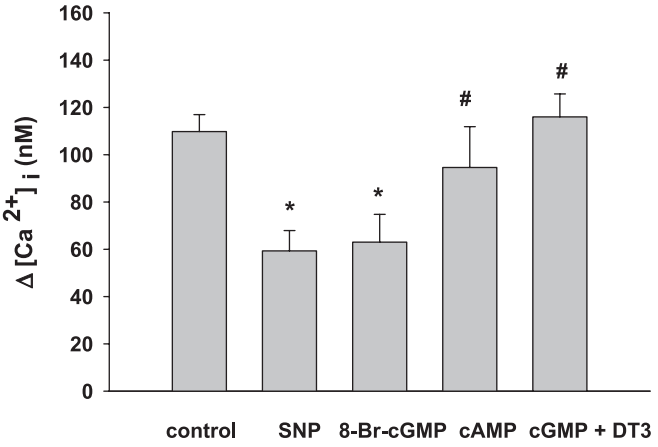

Fig. 2. Bar plots summarizing the effects of SNP, 8-Br-cGMP, db-cAMP, and 8-Br-cGMP plus DT-3 on the SOC response. All values represent the SOC response. *Significantly different from control ($P < 0.05$) using ANOVA plus Student-Newman-Keuls test.. #Significantly different ($P < 0.05$) from the 8-Br-cGMP group.

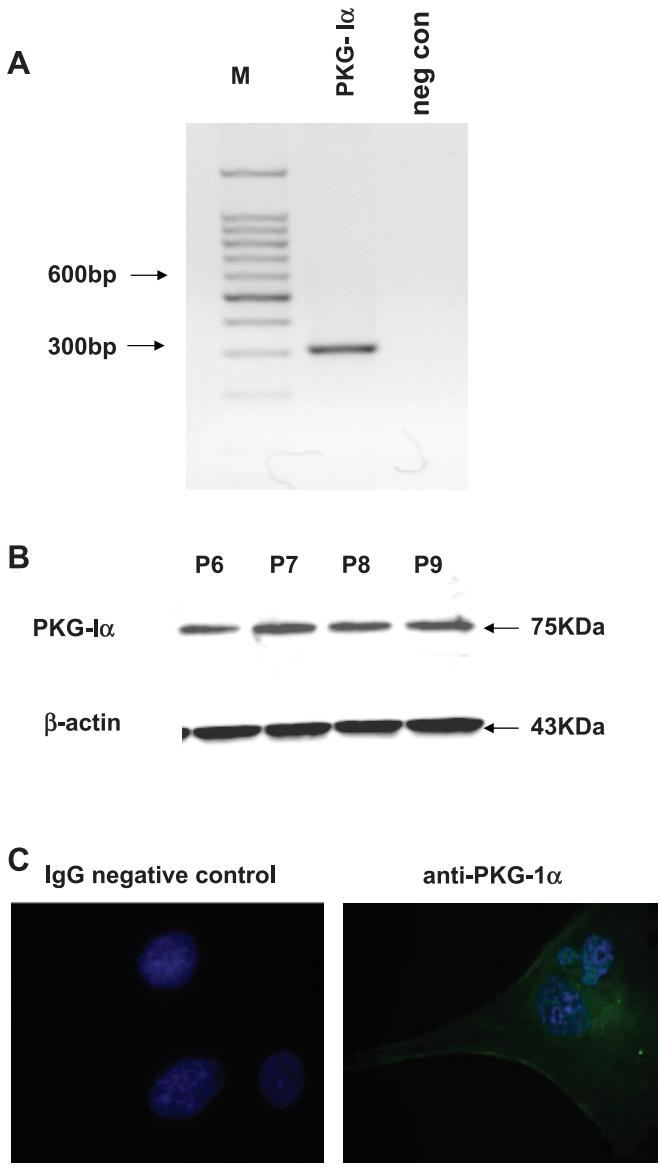

Fig. 3. Detection of PKG-1α protein and transcript in cultured human mesangial cells (HMC). *A*: specific primers and RT-PCR detected mRNA of PKG-α in HMC at 310 bp, the correct size for the designed primers. The second lane is a negative control without the PCR template. The expression quantity of PKG-1α mRNA did not change with *passages 6–9*. *B*: Western blot analysis detected protein of correct size (75 kDa) for PKG-α in HMC. Sample loading was referenced with β-actin. *C*: immunocytochemical localization of PKG-1α. *Left*: IgG negative control. *Right*: anti-PKG-1α.

Detection of PKG-1α in HMC. Previously published pharmacological evidence argues for the presence of PKG in HMC (11, 41, 42, 54). However, the expression of PKG-1α at the message or protein levels in HMC has not been reported. As shown in Fig. 3*A*, PKG-1α-specific primers and RT-PCR detected mRNA at the correct size (310 bp) for our designed PKG-1α primers. Using Western blot analysis (Fig. 3*B*), we detected a protein in HMC near the expected size (75 kDa) for PKG-1α which did not decrease with increasing passage number (*passages 6–9*). Immunocytochemical staining (Fig. 3*C*) shows the presence of light PKG-1α staining throughout the cell. However, prominent staining was at or near the plasma membrane.

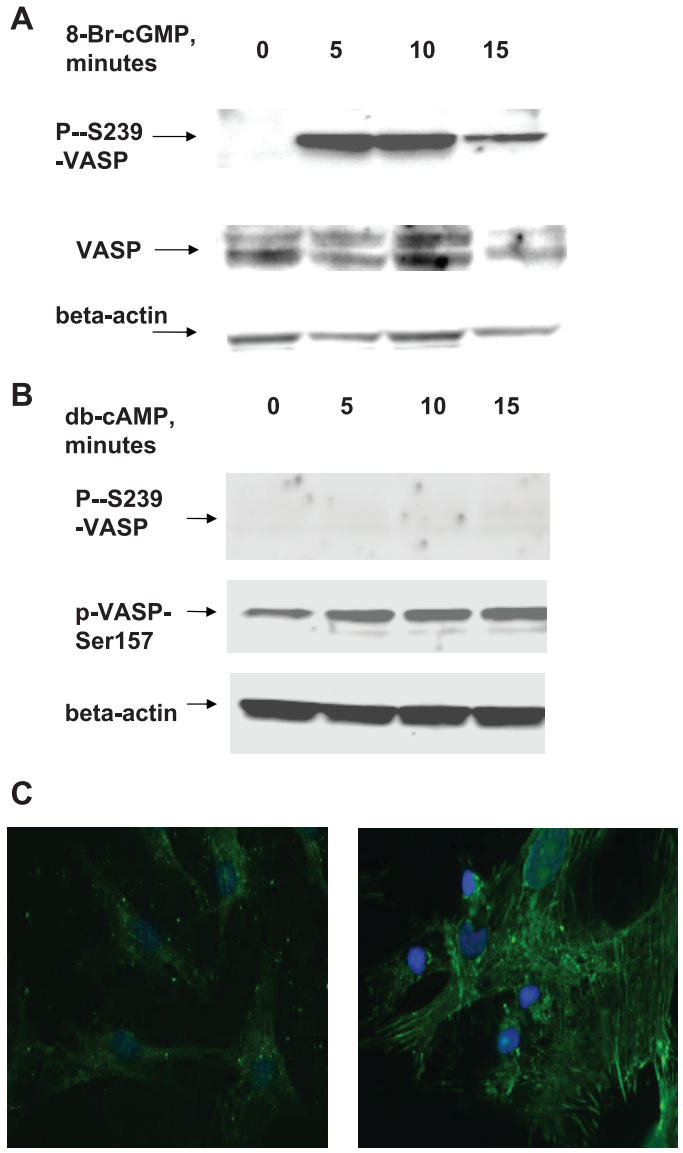

Fig. 4. Time course of phosphorylation of Ser239-vasodilator-stimulated phosphoprotein (VASP) by 8-Br-cGMP. Western blots demonstrating in HMC the time course of phosphorylation of VASP at Ser239 by 8-Br-cGMP (*A*) or db-cAMP (*B*) are shown. 8-Br-cGMP and db-cAMP were applied to 48 h serum-starved HMC at the indicated time points. Sample loading was referenced with β-actin. *C*: immunocytochemical staining with anti-P-Ser239-VASP (green) in HMC incubated with normal media (*left*) or 8-Br-cGMP media (*right*) for 10 min.

VASP is phosphorylated by PKG-1α at Ser239. To demonstrate that the endogenous PKG-1α in HMC is functionally relevant in its response to 100 μM 8-Br-cGMP, we determined with Western blotting the time course of 8-Br-cGMP-stimulated VASP phosphorylation at Ser239. As shown in Fig. 4*A*, exposure of serum-starved HMC to 8-Br-cGMP (100 μM) for 5 min resulted in a substantial increase in P-Ser239-VASP. The expression of total VASP (all phosphorylated and unphosphorylated forms), relative to actin, did not change on addition of 8-Br-cGMP. As shown in Fig. 4*B*, addition of db-cAMP increased the phosphorylation of Ser157-VASP, a known PKA site, but did not cause the phosphorylation of Ser239-VASP. This confirms that Ser239-VASP in HMC is a specific PKG phosphorylation site. Consistent with the Western blot experiments, Fig. 4*C* shows that there is very light staining for P-Ser239-VASP in the absence of 8-Br-cGMP. However, staining appears intense after 10 min of 8-Br-cGMP application. Therefore, the Western blot and the immunocytochemical experiments show that mesangial VASP is phosphorylated at Ser239 after application of 8-Br-cGMP.

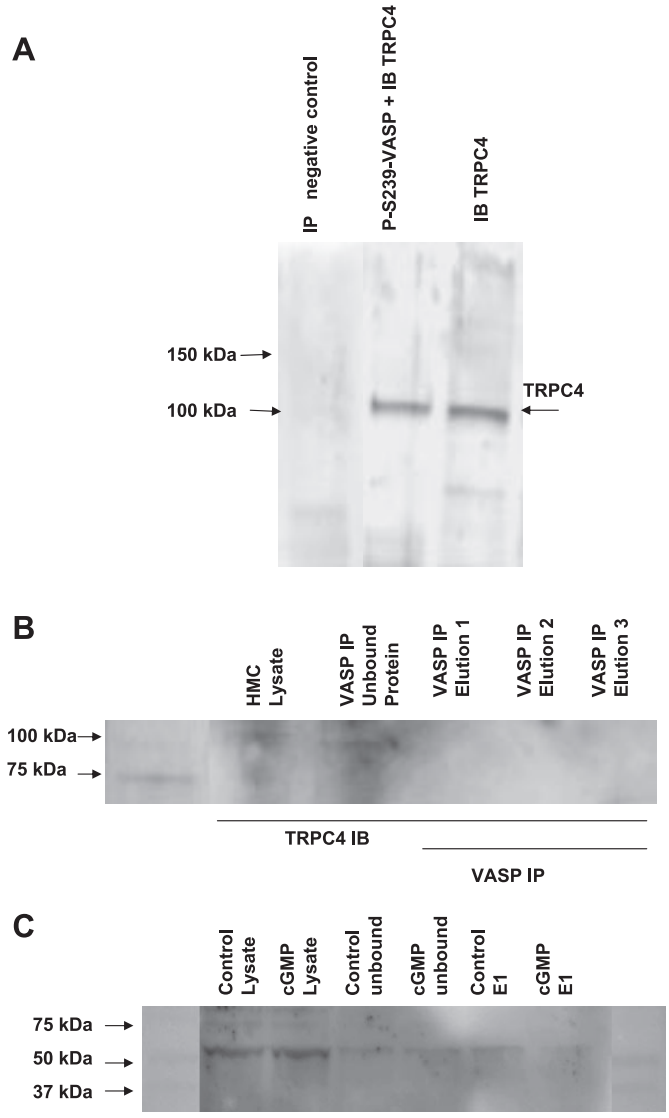

Fig. 5. Association of phosphorylated but not unphosphorylated VASP with TRPC4. *A*: demonstration by coimmunoprecipitation of the association of P-Ser239-VASP with TRPC4 in HMC in the presence of 100 μM cGMP for 10 min. *Lane 1*, negative control [immunoprecipitation (IP) without P- Ser239-VASP]; *lane 2*, IP with P-Ser239-VASP IgG, immunoblotting (IB) with Trpc4 IgG; *lane 3*, IB with Trpc4 IgG. *B*: IP column with (unphosphorylated) anti-VASP IgG (1:20, Calbiochem) and IB with TRPC4 IgG (1:200, Santa Cruz). *Lane 1* reveals TRPC4 in normal control HMC lysate. *Lane 2* shows TRPC4 in the lysate that was unbound after placement in IP column. *Lanes 3*, *4*, and *5* are the different elutions of the protein that was bound to anti-VASP immunoprecipitation column. *C*: positive controls demonstrating the presence of unphosphorylated VASP in HMCs in the absence and presence of 100 μM cGMP. The membrane was blotted with anti-VASP IgG. *Lanes 1* and *2* are normal lysates. *Lanes 3* and *4* are lysates of the protein that remained unbound after placement in the IP column. *Lanes 5* and *6* are the first elution (E1) of the protein that was bound to anti-VASP immunoprecipitation column.

Association of P-Ser239-VASP with TRPC4. It was previously shown that TRPC4 was a component of SOC in mouse MC in culture (60). These experiments were repeated for HMC. As in the previous study, we used the Santa Cruz anti-TRPC4 for all Western blot analysis and immunocytochemical experiments. However, similar immunocytochemical results were obtained with anti-TRPC4 from Alomone (not shown).

As found for mouse mesangial cells, we detected TRPC4 transcript and protein using RT-PCR and Western blotting, respectively (not shown). After repeated attempts, we did not observe phosphorylation of TRPC4 (Western blot detection of anti-phosphoserine proteins) after application of 100 μM 8-Br-cGMP to HMC for 5, 10, 15, and 30 min.

Coimmunoprecipitation was used to determine the association between P-Ser239-VASP and TRPC4 after application of 100 μM 8-Br-cGMP for 10 min. As shown in Fig. 5*A*, TRPC4 IgG recognized a protein associated with P-Ser239-VASP in HMC. However, as shown in Fig. 5*B*, in the absence of cGMP stimulation, TRPC4 IgG did not recognize a protein associated with VASP. Positive controls demonstrating the presence of unphosphorylated VASP in HMC in the absence and presence of 100 μM cGMP are shown in Fig. 5*C*. These coimmunoprecipitation experiments show that TRPC4 associates with P-Ser239-VASP but not VASP, which is unphosphorylated at Ser239.

Coimmunocytochemical staining was used to confirm that P-Ser239-VASP, but not VASP, unphosphorylated at Ser239, was associated with TRPC4. As shown in Fig. 6*A*, costaining with anti-VASP and anti-TRPC4 yielded distinct red and green markers, but not a yellow merge, indicating that these proteins were unassociated. However, as shown in Fig. 6*B*, addition of 8-Br-cGMP for 10 min yielded a yellow merge of the HMC costained with anti-P-Ser239-VASP and anti-TRPC4. Therefore, both coimmunoprecipitation and coimmunocytochemical staining indicate that VASP that is PKG phosphorylated at Ser239, but not unphosphorylated VASP, is associated with TRPC4.

DISCUSSION

The results of this study show that SNP, an NO donor, and 8-Br-cGMP significantly attenuated the SOC response of mesangial cells. This effect was reversed by DT-3, an inhibitor of PKG-1α. RT-PCR and Western blot experiments show that HMC contain endogenous PKG-1α, and the immunocytochemical experiments showed that this enzyme is diffusely localized in the cytoplasm and plasma membrane. TRPC4, a component of the SOC in mesangial cells, was not directly phosphorylated after addition of 8-Br-cGMP. However, 8-Br-cGMP resulted in the phosphorylation of VASP at Ser239, which was associated with TRPC4, a component of the SOC in mesangial cells. As shown by coimmunoprecipitation and coimmunocytochemistry, VASP that was not phosphorylated at Ser239 was not associated with TRPC4. The association of P-Ser239-VASP with TRPC4 suggests that PKG phosphorylation of VASP has a major role in regulating TRPC4/SOC-mediated Ca^{2+} entry in HMC.

Effects of NO and cGMP on SOC. NO is a paracrine and autocrine hormone notable for its relaxant, antiproliferative, and antidedifferentiating effects on vascular smooth muscle cells. In most of its target cells, NO stimulates cytosolic guanylate cyclase which generates intracellular cGMP and stimulates PKG.

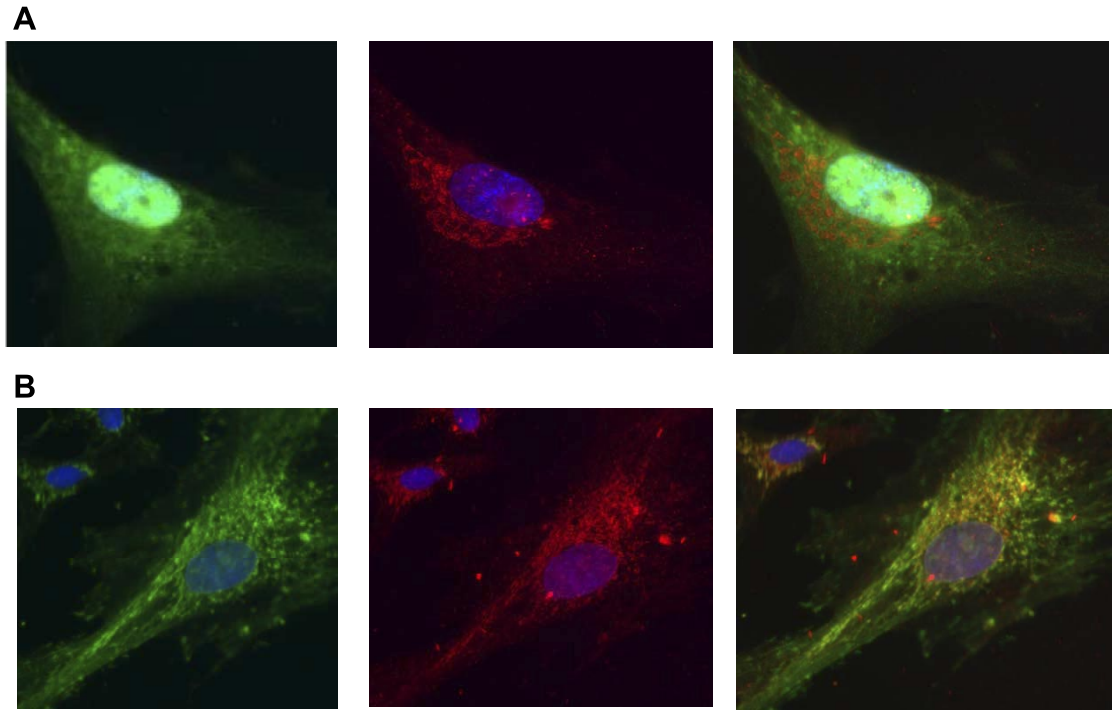

Fig. 6. *A*: coimmunocytochemical staining with anti-VASP and anti-TRPC4 showing pronounced presence of VASP (*left*; green), TRPC4 (*middle*; red), and merge (*right*) in HMC incubated with 10-min application of 8-Br-cGMP. *B*: coimmunocytochemical staining with anti-P-Ser239-VASP (*left*; green) and anti-TRPC4 (*middle*; red), yielding a yellow merge (*right*) in HMC incubated with 10-min application of 8-Br-cGMP.

Several studies have shown that PKG mitigates cellular contractile and proliferative activity by phosphorylating a variety of substrates involved in intracellular Ca^{2+} metabolism. cGMP inhibits store-operated Ca^{2+} entry in airway smooth muscle cells (2), vascular endothelial cells (12, 35), pancreatic acini (63), and human hepatoma cells (29). In human myofibroblastic hepatic stellate cells, C-type natriuretic peptide (which stimulates particulate guanylyl cyclase and elevates intracellular cGMP), inhibited growth and contraction by inhibiting SOC (58).

Elevations in cell [Ca^{2+}] can also modulate cGMP generation. For example, Ca^{2+} entry in the human myometrium increases iNOS-mediated NO production, which then inhibits further Ca^{2+} entry through SOC via a negative feedback mechanism (63). Thus Ca^{2+} and cGMP signaling may constitute two reciprocal limbs of the signaling pathways that govern proliferation.

PKG-α in HMC. In vascular smooth muscle cells, PKG-1α is stimulated by NO-cGMP, which leads to relaxation (56). In this study, PKG-α transcript and protein were identified in HMC by RT-PCR and Western blotting. Although several studies have implied with inhibitors that PKG may be present in MC (11, 54), the present study is the first to identify PKG-1α in HMC. However, because PKG is often expressed at much lower levels than PKA, it is possible that addition of 8-Br-cGMP cross-activated the more abundant PKA. We believe that 8-Br-cGMP specifically activates PKG-1α in HMC because *1*) DT-3, which is a fairly specific inhibitor of PKG-1α, reversed the 8-Br-cGMP-mediated inhibition of SOC activity; and *2*) application of 8-Br-cGMP resulted in a fast phosphorylation of VASP at Ser239, a PKG-specific site. Thus we conclude that PKG-1α is present in HMC and is activated by application of 8-Br-cGMP.

VASP as an intermediary for cGMP-regulated SOC. cGMP regulates, via PKG activation, a variety of ion channels including large, Ca^{2+}-activated K channels (54, 57, 67), CFTR-Cl channels (59), and TRPC3-SOC (34). There are at least two potential PKG phosphorylation sites on TRPC4. However, repeated attempts could not demonstrate direct phosphorylation of TRPC4 by PKG-1α, suggesting that an intermediary protein interacts with TRPC4 and is involved in decreasing TRPC4 activity.

VASP is a focal adhesion molecule highly expressed in mesangial cells (6). VASP has a specific PKG-1α phosphorylation site at Ser239 (52). That 8-Br-cGMP caused an increase in expression of P-Ser239-VASP within 5 min, without affecting VASP expression, indicates the selective activation of PKG.

We are not aware of another study showing an association of VASP with the TRP family of cation channels. However, the adaptor protein Homer forms a cross-linking complex with TRPC1 and IP3R (61, 64). VASP contains the same Ena/VASP homology 1 (EVH1) domain of Homer (4), which interacts with IP3R in the cross-linking complex. It is tempting to speculate that VASP controls the SOC response in MC by cross-linking TRPC4/TRPC1 with IP3R. We hypothesize that, when PKG-1α phosphorylates VASP at Ser239, VASP associates with TRPC4 in the plasma membrane, causing TRPC4 to disengage from the protein complex that comprises the SOC machinery, thereby giving an attenuated SOC response. However, additional studies are required to test this hypothesis.

Although there was not a statistical difference, the initial thapsigargin-induced Ca^{2+} release tended to be lower in the group that was exposed to 8-Br-cGMP. A decrease in Ca^{2+} release would be consistent with the finding that VASP contains homology with the EVH1 of Homer, which binds IP3R.

Significance. NO is antimitogenic and decreases focal adhesion proteins and collagen deposition in vascular smooth muscle as well as glomerular mesangial cells. A possible mechanism for the effects of NO is a reduction in Ca^{2+} cell entry, which plays at least a permissive role in mitogenesis or hypertrophy. Kaur et al. (30) showed a reduction in NO-mediated phosphorylation of focal adhesion molecules of vascular smooth muscle. If the same holds true for mesangial cells, this could be a defensive mechanism used for preventing or counteracting cytokine-stimulated entry of Ca^{2+} into mesangial cells, which would protect the glomerulus from progressive disease.

In conclusion, these data support the notion that NO, through its intracellular mediators, cGMP and PKG-1α, increases the phosphorylation of Ser239-VASP, which associates with TRPC4 and inhibits store-operated Ca^{2+} entry.

GRANTS

This work was supported by National Institutes of Health (NIH) Grants RO1-DK-49461, RO1-DK-73070, and RO1-DK-71014 (to S. C. Sansom), a fellowship from the American Heart Association Heartland Affiliate (no. 0425619Z) to X. Wang, and NIH Cardiovascular Research Training Grant 1T32-HL-0788 (to J. Pluznick).

REFERENCES

1. **Abrass CK.** Diabetic nephropathy. Mechanisms of mesangial matrix expansion. *West J Med* 162: 318–321, 1995.
2. **Ay B, Iyanoye A, Sieck GC, Prakash YS, Pabelick CM.** Cyclic nucleotide regulation of store-operated Ca^{2+} influx in airway smooth muscle. *Am J Physiol Lung Cell Mol Physiol* 290: L278–L283, 2006.
3. **Bear JE, Loureiro JJ, Libova I, Fassler R, Wehland J, Gertler FB.** Negative regulation of fibroblast motility by Ena/VASP proteins. *Cell* 101: 717–728, 2000.
4. **Beneken J, Tu JC, Xiao B, Nuriya M, Yuan JP, Worley PF, Leahy DJ.** Structure of the Homer EVH1 domain-peptide complex reveals a new twist in polyproline recognition. *Neuron* 26: 143–154, 2000.
5. **Blatter LA, Wier WG.** Nitric oxide decreases $[Ca^{2+}]_i$ in vascular smooth muscle by inhibition of the calcium current. *Cell Calcium* 15: 122–131, 1994.
6. **Burkhardt M, Glazova M, Gambaryan S, Vollkommer T, Butt E, Bader B, Heermeier K, Lincoln TM, Walter U, Palmetshofer A.** KT5823 inhibits cGMP-dependent protein kinase activity in vitro but not in intact human platelets and rat mesangial cells. *J Biol Chem* 275: 33536–33541, 2000.
7. **Chen L, Daum G, Chitaley K, Coats SA, Bowen-Pope DF, Eigenthaler M, Thumati NR, Walter U, Clowes AW.** Vasodilator-stimulated phosphoprotein regulates proliferation and growth inhibition by nitric oxide in vascular smooth muscle cells. *Arterioscler Thromb Vasc Biol* 24: 1403–1408, 2004.
8. **Choudhury GG, Biswas P, Grandaliano G, Abboud HE.** Involvement of PKC-α in PDGF-mediated mitogenic signaling in human mesangial cells. *Am J Physiol Renal Fluid Electrolyte Physiol* 265: F634–F642, 1993.
9. **Cohen MP, Clements RS, Hud E, Cohen JA, Ziyadeh FN.** Evolution of renal function abnormalities in the db/db mouse that parallels the development of human diabetic nephropathy. *Exp Nephrol* 4: 166–171, 1996.
10. **Craven PA, Studer RK, Felder J, Phillips S, DeRubertis FR.** Nitric oxide inhibition of transforming growth factor-β and collagen synthesis in mesangial cells. *Diabetes* 46: 671–681, 1997.
11. **de Frutos S, Saura M, Rivero-Vilches FJ, Rodriguez-Puyol D, Rodriguez-Puyol M.** C-type natriuretic peptide decreases soluble guanylate cyclase levels by activating the proteasome pathway. *Biochim Biophys Acta* 1643: 105–112, 2003.
12. **Dedkova EN, Blatter LA.** Nitric oxide inhibits capacitative Ca^{2+} entry and enhances endoplasmic reticulum Ca^{2+} uptake in bovine vascular endothelial cells. *J Physiol* 539: 77–91, 2002.

13. **Dolmetsch RE, Lewis RS, Goodnow CC, Healy JI.** Differential activation of transcription factors induced by Ca^{2+} response amplitude and duration. *Nature* 386: 855–858, 1997.
14. **Du J, Sours-Brothers S, Coleman R, Ding M, Graham S, Kong DH, Ma R.** Canonical transient receptor potential 1 channel is involved in contractile function of glomerular mesangial cells. *J Am Soc Nephrol* 18: 1437–1445, 2007.
15. **Dubey RK.** Vasodilator-derived nitric oxide inhibits fetal calf serum- and angiotensin-II-induced growth of renal arteriolar smooth muscle cells. *J Pharmacol Exp Ther* 269: 402–408, 1994.
16. **Dubey RK, Jackson EK, Lüscher TF.** Nitric oxide inhibits angiotensin II-induced migration of rat aortic smooth muscle cell. Role of cyclic-nucleotides and angiotensin 1 receptors. *J Clin Invest* 96: 141–149, 1995.
17. **Estacion M, Mordan LJ.** Competence induction by PDGF requires sustained calcium influx by a mechanism distinct from storage-dependent calcium influx. *Cell Calcium* 14: 439–454, 1993.
18. **Etienne P, Parés-Herbuté N, Monnier L.** Enhanced antiproliferative effect of nitric oxide in cultured smooth muscle cells from diabetic rats. *J Cardiovasc Pharmacol* 27: 140–146, 1996.
19. **Fantozzi I, Zhang S, Platoshyn O, Remillard CV, Cowling RT, Yuan JX.** Hypoxia increases AP-1 binding activity by enhancing capacitative Ca^{2+} entry in human pulmonary artery endothelial cells. *Am J Physiol Lung Cell Mol Physiol* 285: L1233–L1245, 2003.
20. **Feske S, Gwack Y, Prakriya M, Srikanth S, Puppel SH, Tanasa B, Hogan PG, Lewis RS, Daly M, Rao A.** A mutation in Orai1 causes immune deficiency by abrogating CRAC channel function. *Nature* 441: 179–185, 2006.
21. **Fiedler B, Wollert KC.** Interference of antihypertrophic molecules and signaling pathways with the Ca^{2+}-calcineurin-NFAT cascade in cardiac myocytes. *Cardiovasc Res* 63: 450–457, 2004.
22. **Gambaryan S, Hauser W, Kobsar A, Glazova M, Walter U.** Distribution, cellular localization, and postnatal development of VASP and Mena expression in mouse tissues. *Histochem Cell Biol* 116: 535–543, 2001.
23. **Ghosh TK, Bian JH, Short AD, Rybak SL, Gill DL.** Persistent intracellular calcium pool depletion by thapsigargin and its influence on cell growth. *J Biol Chem* 266: 24690–24697, 1991.
24. **Gomez TM, Robles E.** The great escape; phosphorylation of Ena/VASP by PKA promotes filopodial formation. *Neuron* 42: 1–3, 2004.
25. **Grynkiewicz G, Poenie M, Tsien RY.** A new generation of Ca^{2+} indicators with greatly improved fluorescence properties. *J Biol Chem* 260: 3440–3450, 1985.
26. **Hohenstein B, Kasperek L, Kobelt DJ, Daniel C, Gambaryan S, Renne T, Walter U, Amann KU, Hugo CP.** Vasodilator-stimulated phosphoprotein-deficient mice demonstrate increased platelet activation but improved renal endothelial preservation and regeneration in passive nephrotoxic nephritis. *J Am Soc Nephrol* 16: 986–996, 2005.
27. **Hoshiyama M, Li B, Yao J, Harada T, Morioka T, Oite T.** Effect of high glucose on nitric oxide production and endothelial nitric oxide synthase protein expression in human glomerular endothelial cells. *Nephron Exp Nephrol* 95: e62–e68, 2003.
28. **Ingram AJ, James L, Ly H, Thai K, Cai L, Scholey JW.** Nitric oxide modulates stretch activation of mitogen-activated protein kinases in mesangial cells. *Kidney Int* 58: 1067–1077, 2000.
29. **Jiang JL, Yu MK, Chen ZN, Chan HC.** cGMP-regulated store-operated calcium entry in human hepatoma cells. *Cell Biol Int* 25: 993–995, 2001.
30. **Kaur K, Yao JA, Pan XL, Matthews C, Hassid A.** NO decreases phosphorylation of focal adhesion proteins via reduction of Ca in rat aortic smooth muscle cells. *Am J Physiol Heart Circ Physiol* 274: H1613–H1619, 1998.
31. **Kazerounian S, Pitari GM, Shah FJ, Frick GS, Madesh M, Ruiz-Stewart I, Schulz S, Hajnoczky G, Waldman SA.** Proliferative signaling by store-operated calcium channels opposes colon cancer cell cytostasis induced by bacterial enterotoxins. *J Pharmacol Exp Ther* 314: 1013–1022, 2005.
32. **King AJ, Troy JL, Anderson S, Neuringer JR, Gunning M, Brenner BM.** Nitric oxide: a potential mediator of amino acid-induced renal hyperemia and hyperfiltration. *J Am Soc Nephrol* 1: 1271–1277, 1991.
33. **Kojima I, Mogami H, Shibata H, Ogata E.** Role of calcium entry and protein kinase C in the progression activity of insulin-like growth factor-I in Balb/c 3T3 cells. *J Biol Chem* 268: 10003–10006, 1993.
34. **Kwan HY, Huang Y, Yao X.** Regulation of canonical transient receptor potential isoform 3 (TRPC3) channel by protein kinase G. *Proc Natl Acad Sci USA* 101: 2625–2630, 2004.
35. **Kwan HY, Huang Y, Yao XQ.** Store-operated calcium entry in vascular endothelial cells is inhibited by cGMP via a protein kinase G-dependent mechanism. *J Biol Chem* 275: 6758–6763, 2000.
36. **Kwiatkowski AV, Gertler FB, Loureiro JJ.** Function and regulation of Ena/VASP proteins. *Trends Cell Biol* 13: 386–392, 2003.
37. **Liou J, Kim ML, Heo WD, Jones JT, Myers JW, Ferrell JE Jr, Meyer T.** STIM is a Ca^{2+} sensor essential for Ca^{2+}-store-depletion-triggered Ca^{2+} influx. *Curr Biol* 15: 1235–1241, 2005.
38. **Lucas SS, Lopez-Alcorocho JM, Bartolome J, Carreno V.** Nitric oxide and TGF-beta1 inhibit HNF-4alpha function in HEPG2 cells. *Biochem Biophys Res Commun* 321: 688–694, 2004.
39. **Ma R, Smith S, Child A, Carmines PK, Sansom SC.** Store-operated Ca^{2+} channels in human glomerular mesangial cells. *Am J Physiol Renal Physiol* 278: F954–F961, 2000.
40. **Machesky LM.** Putting on the brakes: a negative regulatory function for Ena/VASP proteins in cell migration. *Cell* 101: 685–688, 2000.
41. **Mene P, Pugliese F, Cinotti GA.** Cyclic nucleotides inhibit Na^+/Ca^{2+} exchange in cultured human mesangial cells. *Exp Nephrol* 1: 245–252, 1993.
42. **Pandey KN, Nguyen HT, Li M, Boyle JW.** Natriuretic peptide receptor-A negatively regulates mitogen-activated protein kinase and proliferation of mesangial cells: role of cGMP-dependent protein kinase. *Biochem Biophys Res Commun* 271: 374–379, 2000.
43. **Rane SG.** Ion channels as physiological effectors for growth factor receptor and Ras/ERK signaling pathways. *Adv Second Messenger Phosphoprotein Res* 33: 107–127, 1999.
44. **Reinhard M, Jarchau T, Walter U.** Actin-based motility: stop and go with Ena/VASP proteins. *Trends Biochem Sci* 26: 243–249, 2001.
45. **Reiser J, Polu KR, Moller CC, Kenlan P, Altintas MM, Wei C, Faul C, Herbert S, Villegas I, Avila-Casado C, McGee M, Sugimoto H, Brown D, Kalluri R, Mundel P, Smith PL, Clapham DE, Pollak MR.** TRPC6 is a glomerular slit diaphragm-associated channel required for normal renal function. *Nat Genet* 37: 739–744, 2005.
46. **Roos J, DiGregorio PJ, Yeromin AV, Ohlsen K, Lioudyno M, Zhang S, Safrina O, Kozak JA, Wagner SL, Cahalan MD, Velicelebi G, Stauderman KA.** STIM1, an essential and conserved component of store-operated Ca^{2+} channel function. *J Cell Biol* 169: 435–445, 2005.
47. **Rupprecht HD, Akagi Y, Keil A, Hofer G.** Nitric oxide inhibits growth of glomerular mesangial cells: role of the transcription factor EGR-1. *Kidney Int* 57: 70–82, 2000.
48. **Rusanescu G, Qi H, Thomas SM, Brugge JS, Halegoua S.** Calcium influx induces neurite growth through a Src-Ras signaling cassette. *Neuron* 15: 1415–1425, 1995.
49. **Sawyer ST, Cohen S.** Enhancement of calcium uptake and phosphatidylinositol turnover by epidermal growth factor in A-431 cells. *Biochemistry* 20: 6280–6286, 1981.
50. **Short AD, Bian J, Ghosh TK, Waldron RT, Rybak SL, Gill DL.** Intracellular Ca^{2+} pool content is linked to control of cell growth. *Proc Natl Acad Sci USA* 90: 4986–4990, 1993.
51. **Shultz PJ, Archer SL, Rosenberg ME.** Inducible nitric oxide synthase mRNA and activity in glomerular mesangial cells. *Kidney Int* 46: 683–689, 1994.
52. **Smolenski A, Bachmann C, Reinhard K, Honig-Liedl P, Jarchau T, Hoschuetzky H, Walter U.** Analysis and regulation of vasodilator-stimulated phosphoprotein serine 239 phosphorylation in vitro and in intact cells using a phosphospecific monoclonal antibody. *J Biol Chem* 273: 20029–20035, 1998.
53. **Sours S, Du J, Chu S, Ding M, Zhou XJ, Ma R.** Expression of canonical transient receptor potential (TRPC) proteins in human glomerular mesangial cells. *Am J Physiol Renal Physiol* 290: F1507–F1515, 2006.
54. **Stockand JD, Sansom SC.** Mechanism of activation by cGMP-dependent protein kinase of large Ca^{2+}-activated K^+ channels in mesangial cells. *Am J Physiol Cell Physiol* 271: C1669–C1677, 1996.
55. **Stockand JD, Sansom SC.** Large Ca^{2+}-activated K^+ channels responsive to angiotensin II in cultured human mesangial cells. *Am J Physiol Cell Physiol* 267: C1080–C1086, 1994.
56. **Surks HK, Mochizuki N, Kasai Y, Georgescu SP, Tang KM, Ito M, Lincoln TM, Mendelsohn ME.** Regulation of myosin phosphatase by a specific interaction with cGMP-dependent protein kinase Ialpha. *Science* 286: 1583–1587, 1999.
57. **Swayze RD, Braun AP.** A catalytically inactive mutant of type I cGMP-dependent protein kinase prevents enhancement of large conductance, calcium-sensitive K^+ channels by sodium nitroprusside and cGMP. *J Biol Chem* 276: 19729–19737, 2001.

58. **Tao J, Mallat A, Gallois C, Belmadani S, Mery PF, Nhieu JT, Pavoine C, Lotersztajn S.** Biological effects of C-type natriuretic peptide in human myofibroblastic hepatic stellate cells. *J Biol Chem* 274: 23761–23769, 1999.
59. **Vaandrager AB, Tilly BC, Smolenski A, Schneider-Rasp S, Bot AGM, Edixhoven M, Scholte BJ, Jarchau T, Walter U, Lohmann SM, Poller WC, De Jonge HR.** cGMP stimulation of cystic fibrosis transmembrane conductance regulator Cl^- channels co-expressed with cGMP-dependent protein kinase type II but not type Iβ. *J Biol Chem* 272: 4195–4200, 1997.
60. **Wang X, Pluznick JL, Wei P, Padanilam BJ, Sansom SC.** TRPC4 forms store-operated Ca^{2+} channels in mouse mesangial cells. *Am J Physiol Cell Physiol* 287: C357–C364, 2004.
61. **Weerth SH, Holtzclaw LA, Russell JT.** Signaling proteins in raft-like microdomains are essential for Ca^{2+} wave propagation in glial cells. *Cell Calcium* 41: 155–167, 2007.
62. **Wei P, Lane PH, Lane JT, Padanilam BJ, Sansom SC.** Glomerular structural and functional changes in a high-fat diet mouse model of early-stage Type 2 diabetes. *Diabetologia* 47: 1541–1549, 2004.
63. **Xu X, Star RA, Tortorici G, Muallem S.** Depletion of Intracellular Ca^{2+} stores activates nitric-oxide synthase to generate cGMP and regulate Ca^{2+} influx. *J Biol Chem* 269: 12645–12653, 1994.
64. **Yuan JP, Kiselyov K, Shin DM, Chen J, Shcheynikov N, Kang SH, Dehoff MH, Schwarz MK, Seeburg PH, Muallem S, Worley PF.** Homer binds TRPC family channels and is required for gating of TRPC1 by IP_3 receptors. *Cell* 114: 777–789, 2003.
65. **Yuan JP, Zeng W, Huang GN, Worley PF, Muallem S.** STIM1 heteromultimerizes TRPC channels to determine their function as store-operated channels. *Nat Cell Biol* 9: 636–645, 2007.
66. **Zhang W, Meng H, Li ZH, Shu Z, Ma X, Zhang BX.** Regulation of STIM1, store-operated Ca^{2+} influx, and nitric oxide generation by retinoic acid in rat mesangial cells. *Am J Physiol Renal Physiol* 292: F1054–F1064, 2007.
67. **Zhou X, Schlossmann J, Hofmann F, Ruth P, Korth M.** Regulation of stably expressed and native BK channels from human myometrium by cGMP- and cAMP-dependent protein kinase. *Pflügers* Arch. 436: 725–734. 2000.